

# Gain-Scheduled Controller Design by Linear Programming with Application to a Double-Axis Positioning System

Marc Kunze, Alireza Karimi and Roland Longchamp

**Abstract**—A linear programming approach is proposed to tune fixed-order linearly parameterized gain-scheduled controllers for stable SISO Linear Parameter Varying (LPV) plants. The method is based on the shaping of the open-loop transfer functions in the Nyquist diagram with constraints on the robustness margins and on the lower approximation of the crossover frequency. Two optimization problems are considered: optimization for robustness and optimization for performance. This method directly computes a gain-scheduled controller from a set of frequency-domain models in different operating points or from an LPV model and no interpolation is needed. In terms of closed-loop performance, this approach leads to extremely good results. However, closed-loop stability is ensured only locally and for slow variations of the scheduling parameters. A stability analysis should be performed for fast variations of the scheduling parameters. An application to a high-precision double-axis positioning system illustrates the effectiveness of the proposed approach.

## I. INTRODUCTION

A large class of nonlinear systems can be represented by a set of linear models that approximate the dynamics of the systems in different operating points. The dynamic behavior of such systems varies as a function of some scheduling parameters. Many electromechanical systems, such as for example component mounters, H-drives and electromagnetic levitation systems belong to this class of systems. For these examples, the scheduling parameter is the position, as their dynamics change as a function of the position.

Such time-varying behavior cannot be controlled by classical linear control methods, as these methods require a Linear Time Invariant (LTI) model of the system. One solution to this problem is to design an LTI controller that is robust against these varying dynamics. In this approach, the variation of the dynamics as a function of the scheduling parameters is treated as uncertainty, which often leads to poor closed-loop performance.

The performance of the controlled system can be improved if the knowledge of the scheduling parameters is included in the controller by making it dependent on these parameters. The corresponding synthesis procedure is commonly referred as gain-scheduling (see the survey papers [1] and [2]). Basically two classes of methods can be distinguished: one is called the classical gain-scheduling methods and the other one the direct Linear Parameter Varying (LPV) controller design methods.

The classical gain-scheduling methods proceed in two steps. First, a finite grid of operating points is chosen within the whole range of operating points and a controller is designed for each of these selected operating points based on the local model. Secondly, an interpolation between the controllers is made to get a gain-scheduled (or LPV) controller. Usually, the gain-scheduled controller is obtained by interpolation between the parameters of the local controllers. However, different methods exist. For example in [3] an affine interpolation between the poles, zeros and gains of the local controllers is made, resulting in an affine state-space representation of the LPV controller. Classical gain-scheduling methods give good closed-loop performance and are simple to use: no LPV model is needed; controllers can be designed easily using for example a classical loop-shaping method; the implementation of the controller is straightforward. The major drawback lies in the fact that the global stability of the closed-loop system is not always assured, in particular for fast variations of the scheduling parameters.

Direct LPV controller design methods are based on LPV models. These approaches are different from the classical gain-scheduling methods since they involve the direct synthesis of a controller rather than its construction from a family of local linear controllers designed by LTI methods. The direct methods can be divided into two main categories: methods using a small-gain Linear Fractional Transformation (LFT) approach [4] and methods using a Lyapunov-based approach [5]. The major advantage of these methods is that they assure the global stability of the closed-loop system. Unfortunately, they are more conservative than the classical gain-scheduling methods, leading to poorer closed-loop performance. Moreover, as mentioned in [6], they are often affected by numerical conditioning and by practical implementation problems.

In this paper, a classical gain-scheduling method is proposed based on an extension of the linear programming method presented in [7]. The proposed method tunes fixed-order linearly parameterized gain-scheduled controllers for stable LPV plants by shaping the open-loop transfer functions in the Nyquist diagram. This method is one shot in the sense that a gain-scheduled (or LPV) controller is directly computed from an LPV model or a set of models in different operating points and no interpolation step is required. A linear stability margin, which guarantees for the frozen parameters a lower bound for the gain, phase and modulus margins and a lower approximation of the crossover frequency are used as constraints. These constraints are linear with respect to

the parameters of the linearly parameterized controller. Thus, an optimization problem that maximizes the robustness or the closed-loop performance in terms of load disturbance rejection, output disturbance rejection and tracking can be solved by linear programming. Since the approach is based on the robust stability, only local stability is guaranteed. Global stability can be considered a posteriori and is also the subject of another work.

This paper is organized as follows. In Section II the class of models and controllers are defined and a summary of the linear programming method presented in [7] is given. Section III shows the extensions to design gain-scheduled controllers. Simulation results are given in Section IV. The proposed method is applied to a double-axis Linear Permanent Magnet Synchronous Motor (LPMSM) in Section V where a stability analysis is also performed. Finally, Section VI gives some concluding remarks.

## II. PRELIMINARIES AND PROBLEM FORMULATION

### A. Plant model

The class of SISO LPV systems, varying according to a  $n_\theta$ -dimensional vector  $\theta$  of scheduling parameters, is considered. The linear systems for frozen scheduling parameters are supposed to have no Right Half-Plane (RHP) pole. It is assumed that a set of non-parametric models in the frequency domain is available. This set is obtained by doing several identification experiments for different values of  $\theta$ . Suppose that the dynamics of the system can be captured by a sufficiently large finite number of frequency points  $N$  and that a sufficiently large number of models  $m$  is available to have a fine grid with respect to  $\theta$ . Then, the set can be presented by:

$$\mathcal{M} = \{G(j\omega_k, \theta_l) \mid k = 1, \dots, N; l = 1, \dots, m\}, \quad (1)$$

where  $\omega_k$  and  $\theta_l$  are, respectively, particular values of the frequency  $\omega$  and of the scheduling parameters  $\theta$ .

### B. Controller parameterization

A class of linearly parameterized controllers is considered:

$$K(s, \theta) = \rho^T(\theta)\phi(s), \quad (2)$$

where

$$\rho^T(\theta) = [\rho_1(\theta), \rho_2(\theta), \dots, \rho_{n_p}(\theta)], \quad (3)$$

$$\phi^T(s) = [\phi_1(s), \phi_2(s), \dots, \phi_{n_p}(s)], \quad (4)$$

$n_p$  is the dimension of  $\rho$  and  $\phi_i(s)$ ,  $i = 1, \dots, n_p$ , are rational basis functions with no RHP pole. As the aim is to design an LPV controller, the controller parameters depend on  $\theta$  (see (3)). Let us assume that  $\rho_i(\theta)$  is a polynomial in  $\theta$  of order  $p_c$ , i.e.:

$$\rho_i(\theta) = (\rho_{i,p_c})^T \theta^{p_c} + \dots + (\rho_{i,1})^T \theta + (\rho_{i,0})^T \vec{1}, \quad (5)$$

where  $\vec{1}$  is an  $n_\theta$ -dimensional vector of ones and  $\theta^k$  denotes element-by-element power of  $k$  of vector  $\theta$ . Thus, the controller is completely characterized by the real vectors  $\rho_{i,p_c}$ ,  $\dots$ ,  $\rho_{i,1}$ ,  $\rho_{i,0}$ .

As an example, the parameterization of a PID controller depending on a scalar  $\theta$  could take the following form:

$$\rho^T(\theta) = [K_p(\theta), K_i(\theta), K_d(\theta)], \quad (6)$$

$$\phi^T(s) = [1, \frac{1}{s}, \frac{s}{1+Ts}], \quad (7)$$

where  $T$  (known) is the time constant of the noise filter. The parameters could be polynomials in  $\theta$  of order 2:

$$K_p(\theta) = K_{p,2}\theta^2 + K_{p,1}\theta + K_{p,0}, \quad (8)$$

$$K_i(\theta) = K_{i,2}\theta^2 + K_{i,1}\theta + K_{i,0}, \quad (9)$$

$$K_d(\theta) = K_{d,2}\theta^2 + K_{d,1}\theta + K_{d,0}, \quad (10)$$

### C. Summary of the linear programming method

Classical gain, phase and modulus margins (radius of the circle centered in  $[-1, j0]$  and tangent to the Nyquist plot of the open-loop transfer function) as well as crossover frequency  $\omega_c$  are nonlinear functions of the controller parameters. Optimization methods with constraints on these values lead to non-convex optimization problems. The linear programming method introduces a new stability margin and a lower approximation of the crossover frequency which lead to linear constraints for an optimization problem in which robustness or performance are maximized [7]. This optimization problem can be solved efficiently by a linear programming method. The following is a summary and the reader can see [7] to have a full description of the method.

1) *Linear robustness margin*: Consider a straight line  $d_1$  in the complex plane crossing the negative real axis between 0 and -1 with an angle  $\alpha \in (0^\circ, 90^\circ]$  (see Fig. 1). The linear stability margin  $\ell \in (0, 1)$  is the distance between the critical point -1 and  $d_1$  where it crosses the negative real axis. If the Nyquist plot of the open-loop transfer function lies on the right-hand side of  $d_1$ , a lower bound on the conventional robustness margins is ensured.

2) *Lower approximation of the crossover frequency*: Consider another straight line  $d_2$  in the complex plane tangent to the unit circle centered at the origin which crosses the negative real axis with an angle  $\beta$  (see Fig. 1). The part of  $d_2$  between  $d_1$  and the imaginary axis is a linear approximation of the unit circle in this region. Now, assume that the open-loop Nyquist plot intersects  $d_2$  at a frequency called  $\omega_x$ . From Fig. 1 it is clear that the crossover frequency  $\omega_c$  is always greater than or equal to  $\omega_x$ . Hence,  $\omega_x$ , which is a lower approximation of the crossover frequency, can be used as a measure of the time-domain performance or the closed-loop bandwidth.

3) *Optimization for robustness*: Optimizing the robustness consists of maximizing the linear robustness margin  $\ell$ .

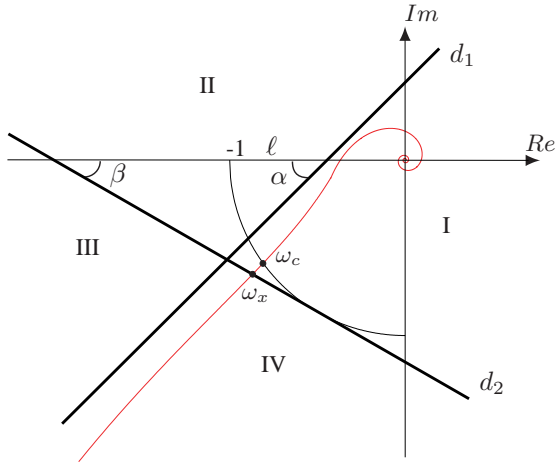


Fig. 1. Linear constraints for robustness and performance, with four regions: I, II, III and IV. The linear stability margin, the crossover frequency and the lower approximation of the crossover frequency are, respectively,  $\ell$ ,  $\omega_c$  and  $\omega_x$ .

4) *Optimization for performance*: Optimizing the load disturbance rejection is considered as the desired performance for the closed-loop system. In general, to reject low-frequency disturbances, the controller gain at low-frequencies should be maximized. For a rational continuous-time controller of order  $n_c$  with fixed denominator  $K_d(s)$ ,

$$K(s, \theta) = \frac{k_{n_c}(\theta)s^{n_c} + \dots + k_1(\theta)s + k_0(\theta)}{K_d(s)}, \quad (11)$$

it corresponds to maximizing  $k_0(\theta)$ . According to (2),  $k_0(\theta)$  is a linear combination of the parameters of the linearly parameterized controller:

$$k_0(\theta) = \sum_{i=1}^{n_p} \gamma_i \rho_i(\theta), \quad (12)$$

where  $\gamma_i$  are the coefficients of the linear combination which depend on the basis functions. For the particular case of  $K_d(s)$  containing only one integrator, maximizing  $k_0(\theta)$  corresponds to minimizing the Integrated Error (IE) caused by a load disturbance [8]:

$$\text{IE} = \int_0^{\infty} e(t) dt \propto \frac{1}{k_0(\theta)}, \quad (13)$$

where  $e(t)$  is the difference between the desired output and the measured output at time  $t$ .

It should be noted that by maximizing  $k_0(\theta)$  not only the IE of the load disturbance rejection is minimized but also the IE of the output disturbance rejection and the IE of the tracking.

### III. EXTENSION TO DESIGN LPV CONTROLLERS

When a set of non-parametric models is available, the parameterization of the controller (see (2)) allows us to write every point on the Nyquist plot of the open-loop  $L(j\omega, \theta_l) = K(j\omega, \theta_l)G(j\omega, \theta_l)$  as a linear function of the parameters of

the vectors  $\rho_{i,p_c}, \dots, \rho_{i,1}, \rho_{i,0}$ :

$$\begin{aligned} K(j\omega_k, \theta_l)G(j\omega_k, \theta_l) &= \rho^T(\theta_l)\phi(j\omega_k)G(j\omega_k, \theta_l) \\ &= \rho^T(\theta_l)\mathcal{R}(\omega_k, \theta_l) + j\rho^T(\theta_l)\mathcal{I}(\omega_k, \theta_l) \\ &= (M\bar{\theta}_l)^T\mathcal{R}(\omega_k, \theta_l) + j(M\bar{\theta}_l)^T\mathcal{I}(\omega_k, \theta_l), \end{aligned} \quad (14)$$

where

$$M = \begin{bmatrix} (\rho_{1,p_c})^T & \dots & (\rho_{1,1})^T & (\rho_{1,0})^T \\ \vdots & \ddots & \vdots & \vdots \\ (\rho_{n_p,p_c})^T & \dots & (\rho_{n_p,1})^T & (\rho_{n_p,0})^T \end{bmatrix}, \quad (15)$$

$$\bar{\theta}_l = [\theta_l^{p_c} \quad \dots \quad \theta_l \quad \mathbf{1}]^T, \quad (16)$$

$\mathcal{R}(\omega_k, \theta_l)$  and  $\mathcal{I}(\omega_k, \theta_l)$  are, respectively, the real and the imaginary parts of  $\phi(j\omega_k)G(j\omega_k, \theta_l)$ .

Before explaining two different optimization problems, it should be noted that the number of integral terms in the open-loop transfer function  $L(s, \theta_l)$  determines where the low frequency points of  $L(s, \theta_l)$  are located. For example, if  $L(s, \theta_l)$  contains two integral terms, the low frequency part of the Nyquist diagram will be located in region III (see Fig. 1). The number of integral terms will determine the constraints of the optimization problems. For this reason, the LPV plants considered should have a fixed number of integral terms.

#### A. Optimization for robustness

In this part, it is supposed that a desired crossover frequency  $\omega_c$  is given and the objective is to find the best controller in terms of the robustness margins. The design variables for the optimization problem are  $\omega_x$ ,  $\alpha$  and  $\beta$ . To guarantee an achieved crossover frequency greater than the desired one,  $\omega_x$  is chosen equal to  $\omega_c$ . The design method is the same whether the open-loop transfer function  $L(s, \theta_l)$  contains one or two integrators. The Nyquist diagram of  $L(j\omega, \theta_l)$  at very low frequencies is located in region III or IV and at very high frequencies in region I (see Fig. 1). In order to ensure a certain distance from the critical point, the Nyquist curve should not enter region II. On the other hand, the Nyquist curve necessarily intersects  $d_2$  at  $\omega_x$ . As a result, the open-loop Nyquist curve  $L(j\omega, \theta_l)$  should lie in region III or IV for frequencies less than  $\omega_x$  and in region I for frequencies greater than  $\omega_x$ . Thus, the following linear optimization problem is considered:

$$\begin{aligned} &\max_M \ell \\ \text{s. t. } & (M\bar{\theta}_l)^T (\cot \alpha \mathcal{I}(\omega_k, \theta_l) - \mathcal{R}(\omega_k, \theta_l)) + \ell \leq 1 \\ & \quad \text{for } \omega_k > \omega_x, \quad l = 1, \dots, m, \\ & (M\bar{\theta}_l)^T (\cos \beta \mathcal{I}(\omega_k, \theta_l) + \sin \beta \mathcal{R}(\omega_k, \theta_l)) > -1 \\ & \quad \text{for } \omega_k > \omega_x, \quad l = 1, \dots, m, \\ & (M\bar{\theta}_l)^T (\cos \beta \mathcal{I}(\omega_k, \theta_l) + \sin \beta \mathcal{R}(\omega_k, \theta_l)) \leq -1 \\ & \quad \text{for } \omega_k \leq \omega_x, \quad l = 1, \dots, m. \end{aligned} \quad (17)$$

The first and second lines correspond to the constraints that the Nyquist curve has to be below  $d_1$  for  $\omega_k > \omega_x$ , the third and fourth lines correspond to the constraints that the Nyquist

curve has to be above  $d_2$  for  $\omega_k > \omega_x$  and the fifth and sixth lines correspond to the constraints that the Nyquist curve has to be below  $d_2$  for  $\omega_k \leq \omega_x$ .

### B. Optimization for performance

Another control objective is to consider some constraints for the robustness margins and maximize the closed-loop performance in terms of the load disturbance rejection, output disturbance rejection and tracking. This can be done by maximizing

$$\min_{l=1, \dots, m} \sum_{i=1}^{n_p} \gamma_i \rho_i(\theta_l). \quad (18)$$

The design variables are limited to the linear robustness margin  $\ell$  and  $\alpha$ . When  $L(s, \theta_l)$  contains only one integrator, the open-loop Nyquist curve should lie in region I or IV. Thus a simple optimization problem can be defined as follows:

$$\begin{aligned} & \max_M K_{\min} \\ \text{s. t. } & (M\bar{\theta}_l)^T (\cot \alpha \mathcal{I}(\omega_k, \theta_l) - \mathcal{R}(\omega_k, \theta_l)) + \ell \leq 1 \\ & \text{for all } \omega_k, \quad l = 1, \dots, m, \\ & \sum_{i=1}^{n_p} \gamma_i \rho_i(\theta_l) - K_{\min} \geq 0 \quad \text{for } l = 1, \dots, m, \end{aligned} \quad (19)$$

For the case of two integrators in  $L(s, \theta_l)$ , the constraints should be modified such that  $L(j\omega, \theta_l)$  at low frequencies can be located in region III. This can be obtained using a straight line in the complex plane. The line  $d_2$  can be used again to divide the complex plane in four regions. The Nyquist diagram of  $L(j\omega, \theta_l)$  should lie in region I or IV for the frequencies greater than  $\omega_x$  and in region III or IV for the frequencies less than  $\omega_x$ . Thus, the optimization problem can be formulated as

$$\begin{aligned} & \max_M K_{\min} \\ \text{s. t. } & (M\bar{\theta}_l)^T (\cot \alpha \mathcal{I}(\omega_k, \theta_l) - \mathcal{R}(\omega_k, \theta_l)) + \ell \leq 1 \\ & \text{for } \omega_k > \omega_x, \quad l = 1, \dots, m, \\ & (M\bar{\theta}_l)^T (\cos \beta \mathcal{I}(\omega_k, \theta_l) + \sin \beta \mathcal{R}(\omega_k, \theta_l)) \leq -1 \\ & \text{for } \omega_k \leq \omega_x, \quad l = 1, \dots, m, \\ & \sum_{i=1}^{n_p} \gamma_i \rho_i(\theta_l) - K_{\min} \geq 0 \quad \text{for } l = 1, \dots, m, \end{aligned} \quad (20)$$

where  $\omega_x$  is this time not a lower approximation, but a lower bound for the crossover frequency as it can be located anywhere in region IV, and not necessarily at the intersection with  $d_2$ .

It should be noted that, even if the methodology presented in this paper is for continuous-time controllers, it can be easily adapted to design discrete-time controllers (see experimental results in Section V).

### C. LPV parametric model

When a set of non-parametric models is available, the optimization methods presented above can be directly applied to compute an LPV controller as the number of models and the number of frequency points are finite. On the other hand, if an LPV parametric model is available, the number of models corresponding to different values of the scheduling parameters and the number of frequency points are infinite, leading to an infinite number of linear constraints if using the proposed method. To solve this problem, the first step is to go from an infinite number of frequency points to a finite number of frequency points by gridding the frequency domain. If the gridding of the frequency domain is not desired, it is still possible to use the generalized KYP method proposed in [9] at the cost of more complexity. At this point the number of constraints is still infinite, since the number of models corresponding to different values of the scheduling parameters  $\theta$  is still infinite. This problem can be solved using two different ways:

- Gridding  $\theta$ . If the number of parameters in  $\theta$  is not large, this approach is feasible since the linear programming method handles efficiently a very large number of constraints.
- Discretizing  $\theta$  using a randomized approach [10], [11]. This method allows to get a finite number of constraints. It means that the solution found satisfies the original set of constraints (infinite number of constraints) with a certain probabilistic level.

There are two advantages for the use of LPV models:

- One can use a finer grid on the operating points to be sure that between the identified models the constraints are satisfied.
- The global stability analysis is possible, as it will be shown in Section V.

## IV. SIMULATION RESULTS

The design method is tested on a system having a resonance whose frequency changes as a function of a scheduling parameter  $\theta$ . Consider the following LPV plant model:

$$G(s, \theta) = \frac{\omega_0^2(\theta)}{s^2 + 2\zeta\omega_0(\theta)s + \omega_0^2(\theta)}, \quad (21)$$

where

$$\omega_0(\theta) = 2 + 0.2\theta, \quad (22)$$

$$\zeta = 0.1, \quad (23)$$

$$\theta \in [-1, 1]. \quad (24)$$

This model could represent the dynamics of a mechatronic system, where the frequency of the resonance is a function of the moving mass. The objective is to design a PID controller with the following structure

$$K(s) = \frac{K_d s^2 + K_p s + K_i}{s(1 + Ts)} \quad (25)$$

that maximizes the robustness of the closed-loop system with a crossover frequency of about 3.3 rad/s. This crossover

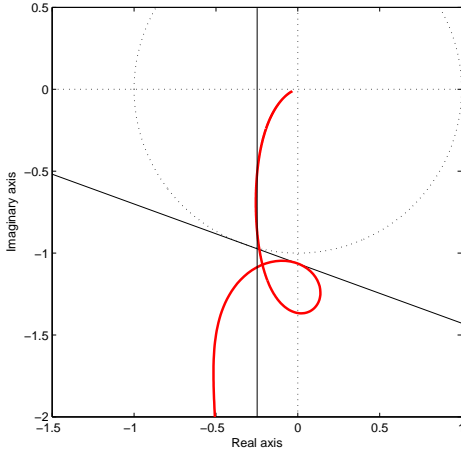


Fig. 2. Nyquist plot of the open-loop transfer function of the PID controller and the nominal model of  $G$ .

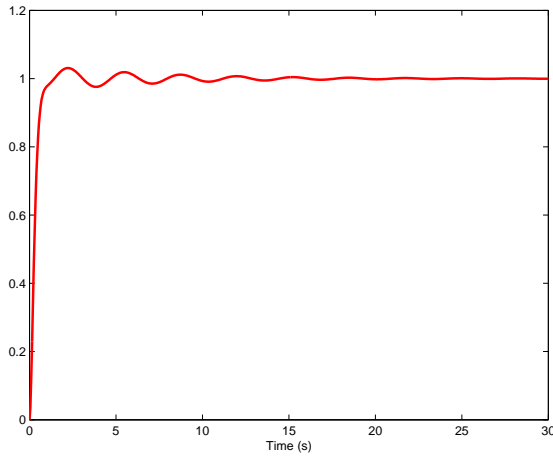


Fig. 3. Set point response of the PID controller and the nominal model of  $G$ .

frequency is chosen because it is about 20% greater than the crossover frequency of the nominal model ( $\theta = 0$ ) in open-loop. The optimization problem (17) is considered. To soften a little bit the constraints, a tolerance on  $\omega_x$  is used, meaning that the frequencies near  $\omega_x$  (up to 2.5 %) can be anywhere and not necessarily in region I, III or IV. The design variable  $\omega_x$  is fixed to 3.3 rad/s,  $\alpha$  to  $90^\circ$  and  $\beta$  to  $20^\circ$ . The time constant  $T$  of the filter of the PID controller is set to 0.1 s.

First, a PID controller is designed for the nominal model. To be able to use the optimization problem (17),  $G(s, 0)$  is evaluated at  $N = 3000$  equally spaced points between 0 and 30 rad/s. The Nyquist plot of the open-loop transfer function obtained by the design is shown in Fig. 2. It can be observed that the Nyquist plot respects the constraints represented by the two lines and leads to a linear margin  $\ell$  of 0.743. The response of the closed-loop system to a set point change is shown in Fig. 3. It can be seen that the response is satisfactory (small overshoot).

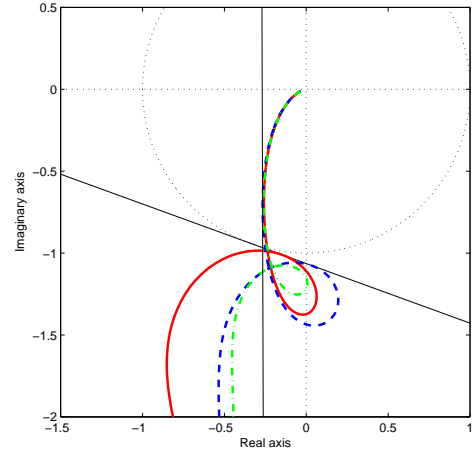


Fig. 4. Nyquist plots of the open-loop transfer functions of the gain-scheduled PID controller and  $G$  for  $\theta = -1$  (solid),  $\theta = 0$  (dashed) and  $\theta = 1$  (dash-dotted).

Now, a robust PID controller is designed for the LPV model. 21 equally spaced discrete values of  $\theta$  are taken between  $-1$  and  $1$ . Once again, for each discretized value  $\theta_l$ ,  $G(s, \theta_l)$  is evaluated at  $N = 3000$  equally spaced points between 0 and 30 rad/s. No solution is obtained from the optimization problem for the whole range of  $\theta$ . A solution is obtained only if  $\theta \in [-0.18, 0.18]$ . This shows the relevance to design a gain-scheduled controller.

Thus, a gain-scheduled PID controller with the following form

$$K(s, \theta) = \frac{1}{s(1 + Ts)} \left[ (K_{d,1}\theta + K_{d,0})s^2 + (K_{p,1}\theta + K_{p,0})s + (K_{i,1}\theta + K_{i,0}) \right] \quad (26)$$

is designed. As it can be seen in (26), the order  $p_c$  of the polynomial in  $\theta$  describing the parameters of the controller is set to 1. As before, 21 equally spaced discrete values of  $\theta$  are taken between  $-1$  and  $1$  and  $G(s, \theta_l)$  is evaluated at  $N = 3000$  equally spaced points between 0 and 30 rad/s. The controller parameters are shown in Table I. The Nyquist plots of the open-loop transfer functions obtained by the design are shown in Fig. 4 for three particular values of  $\theta$  ( $-1$ ,  $0$  and  $1$ ). It can be observed that the Nyquist plots respect the constraints represented by the two lines and lead to a linear margin  $\ell$  of 0.733. The responses of the closed-loop system to a set point change using the gain-scheduled PID controller are shown in Fig. 5 for three frozen particular values of  $\theta$  ( $-1$ ,  $0$  and  $1$ ). It can be seen that the responses to a set point change are very good (small overshoots). The response of the closed-loop system to a set point change using the PID controller designed for the nominal model is also shown in Fig. 5 for  $\theta = -1$ . The response is more oscillatory, which justifies the use of the gain-scheduled controller. Thanks to the gain-scheduled PID controller, it is possible to have about the same performances and robustness for different values of  $\theta$ , which is not possible using a robust PID controller.

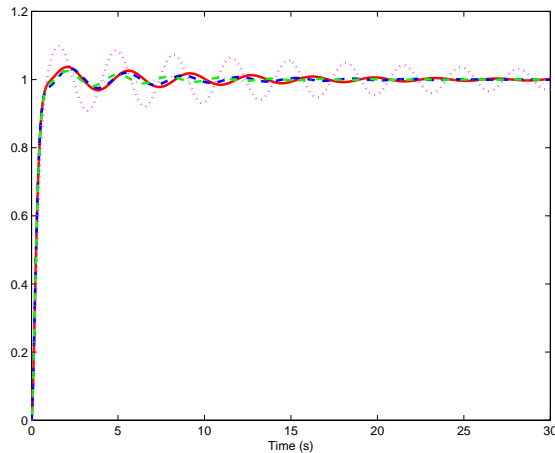


Fig. 5. Set point responses of the gain-scheduled PID controller and  $G$  for  $\theta = -1$  (solid),  $\theta = 0$  (dashed) and  $\theta = 1$  (dashed-dotted) compared to the set point response of the PID controller designed for the nominal model and  $G$  for  $\theta = -1$  (dotted).

TABLE I  
PARAMETERS OF THE GAIN-SCHEDULED PID CONTROLLER.

$K_{d,1}$	$K_{d,0}$	$K_{p,1}$	$K_{p,0}$	$K_{i,1}$	$K_{i,0}$
-0.1832	0.8825	0.0049	0.2156	-0.1017	3.4154

## V. EXPERIMENTAL RESULTS

The gain-scheduled controller design method is applied to a double-axis LPMSM. The objective is to control the position of such a system, which is shown in Fig. 6, using a two-degree of freedom discrete-time controller for each axis operating at a sampling frequency of 18 kHz (imposed by the industrial partner). The design of a precompensator for tracking improvement of this system has been discussed in [12] and in this paper the design of a stabilizing feedback controller is investigated. The advantages of this system are high dynamics (high acceleration and deceleration capabilities), high mechanical stiffness, reduced friction and high accuracy. The high accuracy is due to the fact that it has no mechanical transmission and, therefore, does not suffer from backlash. The particularity of this application is that the dynamics of each axis vary with the position of the two axes. For example, it is clear that the dynamics of the lower axis change as a function of the position of the moving part of the higher axis. If the moving part of the higher axis is at an extremity, it is connected to the lower axis with a different rigidity from the case that the moving part is at the center. Thus, in this application, it is clear that the scheduling parameters are  $x$  and  $y$ , respectively the positions of the higher and lower axes. For reason of brevity, this section will only discuss the model, design of the feedback part of the controller and stability analysis of the higher axis when  $x$  is centered and  $y$  varies from  $-0.16$  m to  $0.16$  m.

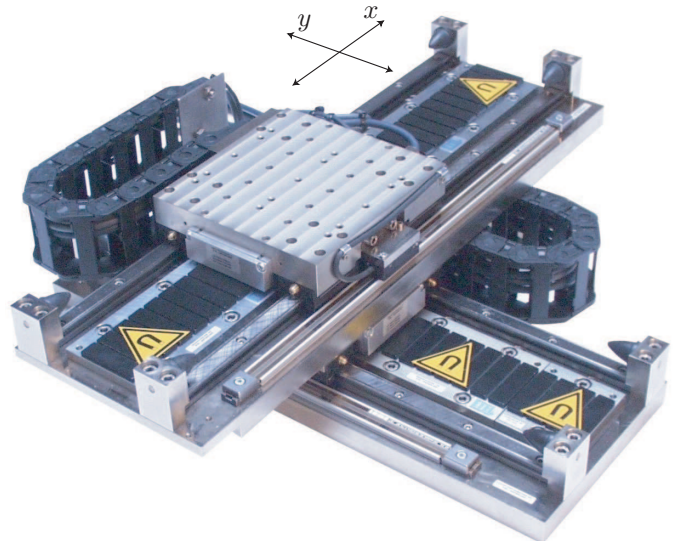


Fig. 6. Double-axis linear permanent magnet synchronous motor (with courtesy of ETEL).

### A. Non-parametric identification of the dynamics of the higher axis

In order to be able to design a gain-scheduled controller for the higher axis, a set of non-parametric models is necessary. To measure the frequency response functions (FRF), the stroke of the lower axis ( $0.32$  m) is divided into 16 equally spaced partitions. The higher axis is positioned at  $x = 0$  m and is excited with a sum of sinusoidal signals from  $4.4$  to  $9000$  Hz for each position of the lower axis and thus, 17 non-parametric models in the frequency domain are obtained. Fig. 7 shows the magnitude Bode diagram of the identified non-parametric models for the higher axis when  $x = 0$  m and  $y$  varies from  $-0.16$  m to  $0.16$  m. This figure shows clearly that the dynamics depend on the position. For low frequencies the higher axis behaves as a single mass system, namely the amplitude plot shows a slope of  $-40$  dB/decade. Between  $100$  and  $140$  Hz, the first decoupling of mass can be seen (zeros, poles). At  $500$  and  $900$  Hz the same phenomenon happens. From  $1000$  Hz, the magnitude Bode diagram is not plotted, since it has mainly a slope of  $-40$  dB/decade with no important informations.

It should be noted that no LPV model is necessary to compute the gain-scheduled controller. This is an advantage as it shortens the procedure of identification.

### B. Gain-scheduled controller design of the higher axis

As a set of non-parametric models is available, it is now possible to design a gain-scheduled controller. The aim is to design a low-order controller that maximizes the robustness with a closed-loop bandwidth of  $180$  Hz (specified by the industrial partner). A gain-scheduled PID controller with the following form

$$K(z^{-1}, y) = \frac{K_n(z^{-1}, y)}{K_d(z^{-1})} \quad (27)$$

with

$$K_n(z^{-1}, y) = k_0(y) + k_1(y)z^{-1} + k_2(y)z^{-2}, \quad (28)$$

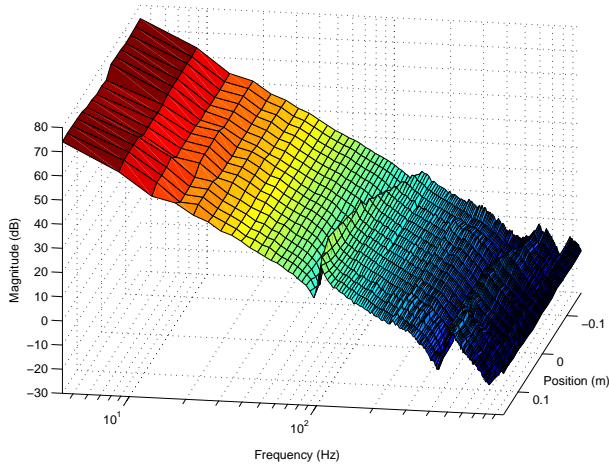


Fig. 7. Magnitude Bode diagram of 17 identified non-parametric models for the higher axis at  $x = 0$  m and  $y = [-0.16:0.02:0.16]$  m.

$$K_d(z^{-1}) = (1 - z^{-1}) \quad (29)$$

is designed, where  $y$  is the scheduling parameter. The order  $p_c$  of the polynomial in  $y$  describing the parameters of the controller is set to 2. To design the controller a modified version of the optimization problem (17) is used. This optimization problem has to be adapted to design discrete-time controller and to deal with the double integrator behavior of the system: as the controller also contains an integral term, the Nyquist diagram has to be located in region II (but very far from the critical point) at very low frequencies. Thus, for the frequencies lower than  $\omega_l$ , the curve is not constrained to be in regions III or IV anymore. Moreover, when the robustness is maximized, this may lead to canceling the integral action of the controller. For a rational discrete-time controller with fixed denominator, the integral action corresponds to the sum of the controller parameters. Thus, to be sure to keep the integral action (which is needed to reject the load disturbances), the following constraints are added:

$$k_0(y) + k_1(y) + k_2(y) \geq K_{\min} \quad (30)$$

for  $y$  in the interval  $[-0.16, 0.16]$  m with increments of 0.02 m. The design variables are  $\omega_x$ ,  $\omega_l$ ,  $\alpha$ ,  $\beta$  and  $K_{\min}$ . The lower approximation of the crossover frequency  $\omega_x$  is set to 180 Hz and  $\omega_l$  to 80 Hz. The value of  $30^\circ$  is used for  $\alpha$  and  $\beta$ . By practical expertise,  $K_{\min}$  is set to 0.004. It should also be noted that, a tolerance of 5 % on  $\omega_x$  is used to soften the constraints, meaning that the frequencies near  $\omega_x$  (up to 5 %) can be anywhere and not necessarily in region I, III or IV.

The Nyquist plots of the open-loop transfer functions obtained by the design are shown in Fig. 8 for three particular values of  $y$  (-0.16 m, 0 m and 0.16 m). It can be observed that the Nyquist plots respect the constraints represented by the two lines and lead to a linear margin  $\ell$  of 0.520.

### C. Stability Analysis

The idea is to analyze the global stability of the higher axis in closed-loop with the designed gain-scheduled controller. To

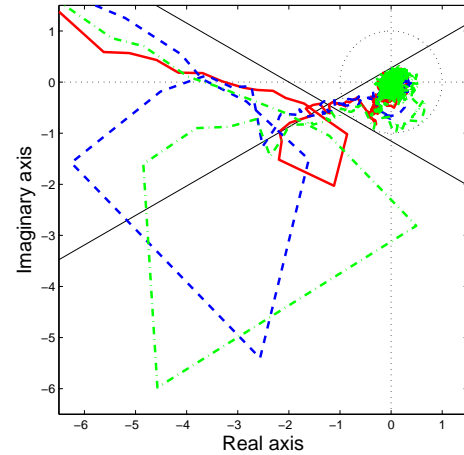


Fig. 8. Nyquist plots of the open-loop transfer functions of the gain-scheduled controller and the system for  $y = -0.16$  m (solid),  $y = 0$  m (dashed) and  $y = 0.16$  m (dashed-dotted).

be able to do it, an LPV parametric model of the higher axis is needed. Since the gain-scheduled controller is designed for  $x$  around 0 m and  $y$  between -0.16 m and 0.16 m, the LPV parametric model is also computed for  $x$  around 0 m and  $y$  between -0.16 m and 0.16 m.

1) *LPV parametric model identification*: In order to compute the LPV parametric model, the procedure proposed by Steinbuch et al. [13] is used, that is: (i) measuring the FRF at different positions giving non-parametric models, (ii) fitting a discrete parametric model on each non-parametric model, (iii) combining these models by linking parameters via a polynomial fit as a function of the position. The first step of the procedure is presented in Subsection V-A. 17 non-parametric models are available at the positions:  $x = 0$  m and  $y$  in the interval  $[-0.16, 0.16]$  m with increments of 0.02 m.

To find parametric models from frequency domain data, the method of Levy is used in continuous-time (see [14] for more details). From Fig. 7 it can be seen that the higher axis has a double integrator behavior as well as three resonances. Only the first one is important for control. Hence, a fourth order continuous-time model is used to fit these curves. Moreover, two poles are set to 0 to represent the double integrator effect. These models are then discretized using a sampling frequency of 2000 Hz (the Nyquist frequency is thus about 10 times greater than the resonance). Fig. 9 shows the Bode diagram of the discrete parametric model at  $x = 0$  m and  $y = 0.14$  m compared to the non-parametric model. It can be observed that the first resonance is well identified. Such a parametric model is computed for the 17 non-parametric models. Thus, the parametric models obtained have the following form:

$$G(z^{-1}) = \frac{b_4 + b_3z^{-1} + b_2z^{-2} + b_1z^{-3} + b_0z^{-4}}{1 + a_3z^{-1} + a_2z^{-2} + a_1z^{-3} + a_0z^{-4}} \quad (31)$$

The last step for the obtention of an LPV model is to combine these models by linking parameters via a polynomial fit as a function of the position. Fig. 10 shows one parameter of the numerator ( $b_0$ ) and one parameter of the denominator ( $a_1$ )

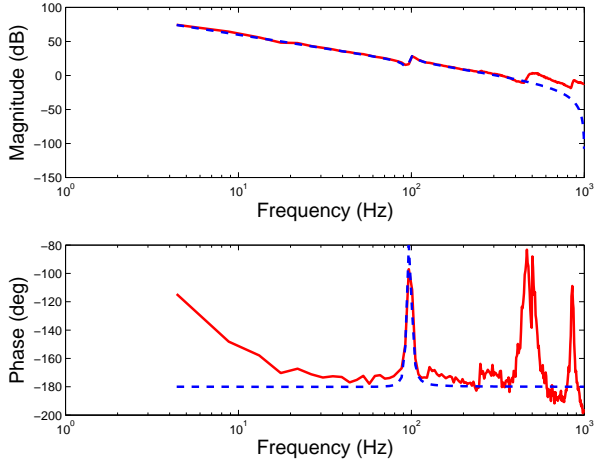


Fig. 9. Bode diagram of the non-parametric (solid) and discrete parametric (dashed) models for the higher axis at  $x = 0$  m and  $y = 0.14$  m.

of the parametric models in function of  $y$  and the polynomials obtained by interpolation. It can be seen that  $a_1$  is well fitted

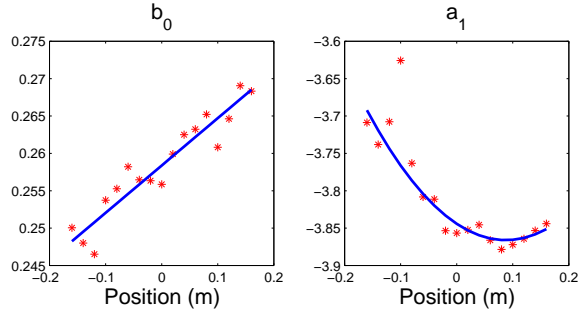


Fig. 10. Parameters of the numerator and denominator of the parametric models for the higher axis in function of  $y$  ( $x = 0$  m and  $y$  is in the interval  $[-0.16, 0.16]$  m with increments of 0.02 m) (star) and polynomials obtained by interpolation (solid line).

by a second-order polynomial. Additionally  $b_0$  is fitted by a linear function. All the parameters of the denominator as well as the parameters of the numerator  $b_1$ ,  $b_2$  and  $b_3$  are also fitted by a second-order polynomial, whereas  $b_4$  is fitted by a linear function. It should be noted that the parametric model obtained for  $y = -0.10$  m does not fit adequately the corresponding non-parametric model, thus it is not taken into account to compute the polynomial fit. Fig. 11 shows the magnitude Bode diagram of the LPV model obtained for the higher axis at  $x = 0$  m and  $y \in [-0.16, 0.16]$  m. It can be observed that this model looks similar to the non-parametric models of Fig. 7, especially the first resonance.

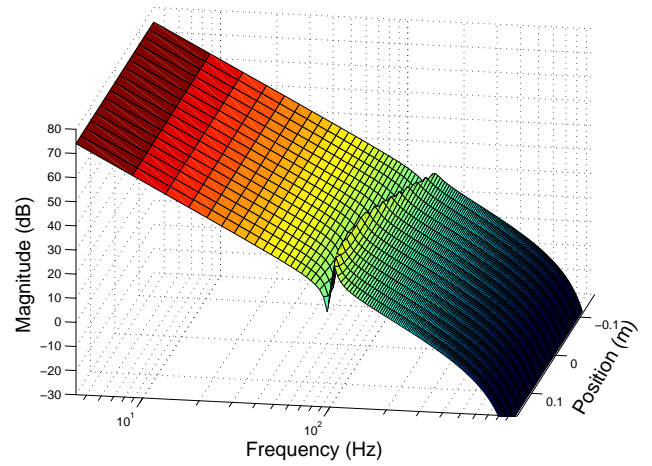


Fig. 11. Magnitude Bode diagram of the LPV model for the higher axis at  $x = 0$  m and  $y \in [-0.16, 0.16]$  m.

2) *Stability analysis using Lyapunov theory:* Once the LPV model is identified, the stability can be analysed. With this objective, Lyapunov stability theory is used. A closed-loop LPV system is globally stable if:

$$\begin{aligned} \exists P > 0 \quad \text{such that:} \\ A(\theta)^T P A(\theta) - P < 0 \quad \forall \theta \end{aligned} \quad (32)$$

Since the number of Linear Matrix Inequalities (LMIs) is infinite, the problem is not directly solvable. If the LPV model can be written in an affine or polytopic form, the number of LMIs is finite. Another solution to solve approximately the problem consists of gridding the scheduling parameter  $\theta$ . Thus, the problem (32) becomes:

$$\begin{aligned} \exists P > 0 \quad \text{such that:} \\ A(\theta_l)^T P A(\theta_l) - P < 0 \quad \text{for } l = 1, \dots, m \end{aligned} \quad (33)$$

If such constraints are satisfied, the LPV system is stable whatever the speed of the scheduling parameter is. For some applications, the maximal speed of the scheduling parameter is known. Thus, this information can be taken into account to reduce the conservatism of the result by using a parameter dependent Lyapunov matrix. Thus, the stability problem becomes:

$$\begin{aligned} \exists P_0 + \theta_l P_1 > 0 \quad \text{for } l = 1, \dots, m \quad \text{such that:} \\ A(\theta_l)^T (P_0 + \theta_{l+n} P_1) A(\theta_l) - (P_0 + \theta_l P_1) < 0 \end{aligned} \quad (34)$$

for  $l = 1, \dots, m$

$n$  is related to the maximal speed of the scheduling parameter i.e. it is the maximal number of discrete scheduling values that can be reached at the next sampling time. In our case, the scheduling parameter is  $y$ , the position of the lower axis. Thus, the closed-loop LPV model is evaluated in 21 equally spaced discrete values of  $y$  between  $-0.16$  m and  $0.16$  m (the controller must be downsampled from 18 kHz to 2000 Hz since the sampling frequency of the LPV model is set to 2000 Hz). Then, the problem (34) is solved recurrently to find the maximal speed for which the system is stable. The stability

could be proven for a motion of 0.08 m with a maximal speed of 9 m/s. For this application, a typical motion has an amplitude of 0.025 m and a maximal speed of 0.5 m/s. Thus, the stability obtained is sufficient.

## VI. CONCLUSIONS

Fixed-order linearly parameterized gain-scheduled controller design is formulated as a linear optimization problem. The proposed method is based on frequency loop shaping in the Nyquist diagram. Classical robustness and performance specifications are represented by linear constraints in the Nyquist diagram. The control objective is to maximize the robustness margin or to maximize the closed-loop performance. This method requires only the frequency response of LPV plants in different operating points and need no interpolation to get the LPV controller, which constitutes a real advantage, since the procedure of designing local controllers and interpolating between them can be very difficult.

Simulation results show that the method can compute a gain-scheduled controller with robustness margins that are unachievable with a classical robust controller.

The application of the proposed method on a system, whose resonance varies as a function of the position, shows that the robustness margins could be improved using a gain-scheduled controller. Moreover, it is shown that it is possible to analyze the stability of the LPV system once the controller is designed.

## REFERENCES

- [1] W. J. Rugh and J. S. Shamma, "Research on gain scheduling," *Automatica*, vol. 36, no. 10, pp. 1401–1425, October 2000.
- [2] D. J. Leith and W. E. Leithead, "Survey of gain-scheduling analysis and design," *International Journal of Control*, vol. 73, no. 11, pp. 1001–1025, July 2000.
- [3] B. Païjmans, W. Symens, H. van Brussel, and J. Swevers, "A gain-scheduling-control technique for mechatronic systems with position-dependent dynamics," in *IEEE American Control Conference*, Minneapolis, Minnesota, USA, June 2006, pp. 2933–2938.
- [4] P. Apkarian and P. Gahinet, "A convex characterization of gain-scheduled  $H_\infty$  controllers," *IEEE Transactions on Automatic Control*, vol. 40, no. 5, pp. 853–864, May 1995.
- [5] G. Becker and A. Packard, "Robust performance of linear parametrically varying systems using parametrically-dependent linear feedback," *Systems & Control Letters*, vol. 23, no. 3, pp. 205–215, 1994.
- [6] M. G. Wassink, M. van de Wal, C. Scherer, and O. Bosgra, "LPV control for a wafer stage: beyond the theoretical solution," *Control Engineering Practice*, vol. 13, no. 2, pp. 231–245, February 2005.
- [7] A. Karimi, M. Kunze, and R. Longchamp, "Robust controller design by linear programming with application to a double-axis positioning system," *Control Engineering Practice*, vol. 15, no. 2, pp. 197–208, February 2007.
- [8] K. J. Åström and T. Hägglund, *Advanced PID Control*. ISA - Instrumentation, Systems, and Automation Society, 2006.
- [9] S. Hara, T. Iwasaki, and D. Shiokata, "Robust PID control using generalized KYP synthesis: Direct open-loop shaping in multiple frequency ranges," *IEEE Control Systems Magazine*, vol. 26, no. 1, pp. 80–91, February 2006.
- [10] G. C. Calafiore and M. C. Campi, "The scenario approach to robust control design," *IEEE Transactions on Automatic Control*, vol. 51, no. 5, pp. 742–753, May 2006.
- [11] Y. Fujisaki, F. Dabbene, and R. Tempo, "Probabilistic design of LPV control systems," *Automatica*, vol. 39, no. 8, pp. 1323–1337, August 2003.
- [12] A. Karimi, M. Butcher, and R. Longchamp, "Model-free precompensator tuning based on the correlation approach," *IEEE Transactions on Control Systems Technology*, vol. 16, no. 5, pp. 1013–1020, September 2008.
- [13] M. Steinbuch, R. van de Molengraft, and A. J. van der Voort, "Experimental modelling and LPV control of a motion system," in *IEEE American Control Conference*, Denver, Colorado, USA, June 2003, pp. 1374–1379.
- [14] R. Longchamp, *Commande numérique de systèmes dynamiques: cours d'automatique*, 2nd ed. Lausanne: Presses Polytechniques et Universitaires Romandes, 2006.